of these authors, combined with the present experiment, indicates that with the use of thick targets the more rapid rate of rise of the cross section above 3.75 Mev is more easily observed. A possible explanation of this effect is the presence of a broad capture resonance at 3.99 Mev. It has been assumed that this is the same resonance which causes the increase in the scattering cross section between 3.6 and 4.0 Mev.

IV. SUMMARY

The measurement of the elastic scattering and capture cross sections of oxygen for protons gives evidence for resonances at proton energies of 2.66, 3.47, 3.99, and 4.39 Mev. The positions of the 2.66- and 3.47-Mev resonances are well determined, while the positions of the upper resonances are based on less substantial evidence. These four resonances correspond to energy levels in the compound nucleus, F^{17}, at 3.11, 3.88, 4.36, and 4.73 Mev.

The authors wish to thank Professor R. G. Herb, under whose supervision this project was carried out, for his advice and encouragement, and Dr. F. P. Mooring for assistance in taking some of the data.

PHYSICAL REVIEW VOLUME 84, NUMBER 1 OCTOBER 1, 1951

Assignment of Angular Momenta to the Energy Levels of F^{17}

R. A. LAUBENSTEIN* AND M. J. W. LAUBENSTEIN*
University of Wisconsin, Madison, Wisconsin†

(Received June 18, 1951)

An analysis of data on the elastic scattering and capture of protons by oxygen was made for the purpose of assigning angular momenta to certain energy levels in F^{17}. The elastic scattering data were analyzed using a graphic method wherein the phase and amplitude of the refracted partial waves are represented by vectors in the complex plane. As the proton energy is varied over a resonance, a circular locus is obtained for the vector which represents the component of a partial wave which excites the resonance.

Assignments of angular momenta to the energy levels of F^{17} have been made as follows: ground state, $D_{\frac{5}{2}}$; 0.55 Mev, $S_{\frac{1}{2}}$; 3.11 Mev, $S_{\frac{1}{2}}$; 3.88 Mev, $F_{\frac{7}{2}}$; 4.36 Mev, $D_{\frac{3}{2}}$; and 4.73 Mev, $P_{\frac{3}{2}}$. The assignments of the 0.55-Mev, 3.11-Mev, and 3.88-Mev levels are reasonably certain, but the others are based on less substantial evidence. The reduced width of the 3.11-Mev $S_{\frac{1}{2}}$ level was found to be about 0.048×10^{-13} Mev-cm, while the 0.55-Mev $S_{\frac{1}{2}}$ level probably has a reduced width over 100 times as large.

The slowly rising capture cross section observed from 1.4 to 3.4 Mev is probably caused by the broad 0.55-Mev level.

A comparison of the levels in the mirror nuclei, O^{17} and F^{17}, shows a similar structure.

I. INTRODUCTION

THERE are a number of reasons to expect that experimental data obtained on the interaction of protons with O^{16} might be more easily interpreted than in the case of many other nuclei. For proton energies below about 5.6 Mev the only reactions which are energetically possible are elastic scattering and simple capture, with capture much less probable. Thus, complications introduced by several competing reactions are avoided. The binding energy of a proton added to an O^{16} nucleus is only 0.61 Mev, which is the lowest positive binding energy observed with any nucleus. Scattering of protons by O^{16}, therefore, gives information about the low-lying levels of F^{17}. Since the lower levels should have larger reduced widths and should be more widely spaced than the upper levels, the problems of experimentally resolving levels and plotting their shapes are less difficult.

Because the spin of O^{16} is zero, the scattering formulas are greatly simplied over the case of non-zero spin, and the results of an elastic scattering experiment should be relatively easy to fit to these formulas. O^{16} contains 8 neutrons and 8 protons and can be considered as a closed shell in both neutrons and protons.[1,2] If this shell model of the nucleus is correct, the compound nucleus, F^{17}, formed under bombardment of O^{16} by protons, will consist of one proton outside a closed shell. The level structure of F^{17} is of theoretical interest because of the possibility of applying this simple nuclear model. Also, O^{17}, the mirror nucleus of F^{17}, has been rather extensively investigated; and it is of interest to compare the levels of these two nuclei.

The results of the previous paper on the elastic scattering and capture of protons by oxygen[3] are far from being sufficiently extensive, so that a detailed theoretical analysis can be made. However, it is interesting to attempt to fit these data to existing formulas, especially in view of the fact that no reaction yield involving a nucleus more complicated than lithium

* Now at North American Aviation, Inc., Downey, California.
† Supported by the Wisconsin Alumni Research Foundation and the AEC.

[1] M. G. Mayer, Phys. Rev. **78**, 16 (1950).
[2] E. Feenberg and K. C. Hammack, Phys. Rev. **75**, 1877 (1949).
[3] Laubenstein, Laubenstein, Koester, and Mobley, Phys. Rev. 84 12 (1951).

has been fitted theoretically over an extended energy range. Because of the lack of sufficient experimental data, many of the conclusions that are reached in this paper must be regarded as tentative; but it is hoped that the interpretation presented here will point the way to further experimental and theoretical work to confirm or deny the conclusions which are reached.

II. ELASTIC SCATTERING THOERY

The cross section for scattering can be given in terms of the phase shifts, δ_l, between the incident and refracted partial waves. For particles of spin $\frac{1}{2}$ incident on nuclei with spin zero, the partial wave which represents particles with l units of orbital angular momentum (measured in units of $\hbar$) must be separated into two components if $l>0$, because of the two possible orientations of the spin with respect to the orbital angular momentum. The phase shift of the component of the lth partial wave which forms a compound state with total angular momentum $J=l+\frac{1}{2}$ will be designated δ_l^+, and the phase shift of the component which forms a compound state with $J=l-\frac{1}{2}$ will be designated δ_l^-. The differential scattering cross section, σ, as a function of these phase shifts, can be obtained from Eqs. (4) and (5) of the paper by Critchfield and Dodder.[4] It is

$$\sigma=\lambda\!\!\!^{-2}[|A|^2+|B|^2], \tag{1}$$

where

$$A=-\tfrac{1}{2}\eta\csc^2\tfrac{1}{2}\theta\exp(i\eta\ln\csc^2\tfrac{1}{2}\theta)+\sum_{l=0}^{\infty}(l+1)P_l(\cos\theta)\exp(i\alpha_l+i\delta_l^+)\sin\delta_l^+ +\sum_{l=1}^{\infty}lP_l(\cos\theta)\exp(i\alpha_l+i\delta_l^-)\sin\delta_l^-, \tag{2}$$

$$B=\sin\theta\sum_{l=1}^{\infty}P_l'(\cos\theta)e^{i\alpha_l}\times[\sin\delta_l^-\exp(i\delta_l^-)-\sin\delta_l^+\exp(i\delta_l^+)], \tag{3}$$

and

$$\eta=ZZ'/\hbar v,\quad \lambda\!\!\!^{-}=\hbar/mv,$$
$$e^{i\alpha_l}=(l+i\eta)/(l-i\eta)\cdots(1+i\eta)/(1-i\eta);\quad l>0$$
$$e^{i\alpha_0}=1,\quad P_l'(\cos\theta)=d[P_l(\cos\theta)]/d(\cos\theta),$$

Z=charge of the proton, Z'=charge of the target nucleus, v=velocity of relative motion, m=reduced mass of the system, and θ=angle of scattering in the center-of-mass system.

The first term in the equation for A (Eq. 2) represents Rutherford or coulomb-type scattering. The other terms in the equations for A and B represent scattering due to nuclear or short-range forces. The phase shifts, δ_l, can be considered, as was done by Adair,[5] to be the sum of a phase shift, $-\phi_l$, due to a hard sphere type of scattering, and of an anomalous phase shift, β_l, due to the energy levels of the compound nucleus. δ_l is then given by

$$\delta_l^+=\beta_l^+-\phi_l,\quad \delta_l^-=\beta_l^--\phi_l,$$

where

$$\phi_l=[\tan^{-1}(F_l/G_l)]_{r=R_l}$$

and $\tan\beta_l^+$ or $\tan\beta_l^-$ is a sum of terms of the form,

$$\tfrac{1}{2}\Gamma_\lambda/(E_\lambda+\Delta_\lambda-E).$$

The sum for $\tan\beta_l^+$ will include only those terms due to resonances caused by energy levels in the compound nucleus which have $J=l+\frac{1}{2}$ and which are formed by protons with l units of orbital angular momentum. Similarly, the sum for $\tan\beta_l^-$ will include only those terms due to resonances caused by energy levels which have $J=l-\frac{1}{2}$ and which are formed by protons with l units of orbital angular momentum. The notation is as follows:[6]

$$\Gamma_\lambda=2k\gamma_\lambda^2/(F_l^2+G_l^2)|_{r=R_l}, \tag{4}$$

$$\Delta_\lambda=-(\gamma_\lambda^2/R_l)[\{d\ln(F_l^2+G_l^2)^{\frac{1}{2}}/d\ln(kr)\}+l]_{r=R_l}, \tag{5}$$

where k=wave number of relative motion, r=distance between the proton and the oxygen nucleus, R_l=effective nuclear radius or reaction radius for the lth partial wave, γ_λ^2=reduced width of the λth level, Δ_λ=level shift of the λth level, E=energy in the center-of-mass system, E_λ=characteristic energy of the λth resonance, and F_l and G_l are the regular and irregular particle wave functions, respectively.[7] If the difference between the incident proton energy and the energy of each resonance excited by l-protons is large compared with the width of that resonance, then it follows that

$$\beta_l^+=\beta_l^-=0,$$

and

$$\delta_l^+=\delta_l^-=-\phi_l.$$

A geometric interpretation of the cross section formula can be obtained by representing the amplitude and phase of each partial wave component by a vector in the complex plane. Adding these vectors to the Rutherford vector gives the resultant A. B can be obtained in a similar manner, but frequently this term is very small compared with A and can be neglected. Because protons scattered near the backward direction were observed in the present experiment,[3] $\sin\theta$ is small and B will be neglected in an analysis of the data. B is, in general, always zero except at energies near a resonance for which $l>0$. Also, at energies which are distant from all resonances except those excited by the lth partial wave, B is zero at those scattering angles for which $P_l'(\cos\theta)$ is zero.

[4] C. L. Critchfield and D. C. Dodder, Phys. Rev. **76**, 602 (1949).
[5] R. K. Adair, Phys. Rev. **81**, 310 (1951).
[6] R. G. Thomas, Phys. Rev. **81**, 148 (1951).
[7] Coulomb wave functions are tabulated in the following papers: Yost, Wheeler, and Breit, Terr. Mag. and Atmos. Elect. **40**, 443 (1935). E. R. Wicher, Terr. Mag. and Atmos. Elect. **41**, 389 (1936). Bloch, Hull, Broyles, Bouricius, Freeman, and Breit, *Coluomb Functions for Reactions of Protons and Alpha Particles with the Lighter Nuclei* (Yale University, New Haven, Connecticut, 1950).

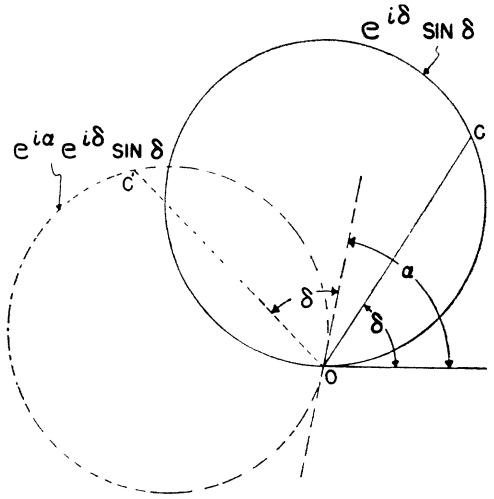

FIG. 1. Representation of terms in the scattering equation by vectors in the complex plane.

If an equation of the form $z=e^{i\delta}\sin^{\delta}$ is plotted in the complex plane, a circle is obtained which passes through the origin and has its center at the point $(0, i/2)$. Such a plot is shown by the solid circle in Fig. 1. The vector OC in this figure is the vector $e^{i\delta}\sin\delta$; and as δ varies from 0° to 180°, the point C will travel counterclockwise once around the circle.[8] Partial waves for which $l>0$ have vectors which are rotated through an additional angle α_l. The dashed circle in Fig. 1 shows that the effect of the $e^{i\alpha l}$ factor in the cross section formula is to rotate the lth locus circles about the origin through an angle α_l. As the $P_{\frac{1}{2}}$ vector is given by $P_1(\cos\theta)\times\exp(i\alpha_1+i\delta_1^-)\sin\delta_1^-$, the vector OC' of Fig. 1 will represent the $P_{\frac{1}{2}}$ vector if $\delta_1^-=\delta$, $\alpha_1=\alpha$, and $\cos\theta>0$. The diameter of the locus circle is given by $(l+1)P_l(\cos\theta)$ for the l^+ partial wave and by $lP_l(\cos\theta)$ for the l^- partial wave.

If the incident proton energy is varied through a resonance, then the term $\beta=\tan^{-1}[\frac{1}{2}\Gamma/(E_\lambda+\Delta_\lambda-E)]$ which is caused by this resonance will vary from near 0° to near 180°. The corresponding vector will travel once around its locus circle. If the angular momentum of the compound state which causes the resonance is J, then the diameter, b, of the locus circle will be $(J+\frac{1}{2})P_l(\cos\theta)$. The ends of the maximum and minimum A vectors will fall at opposite ends of a diameter of the circle; and this diameter, or an extension thereof, will pass through the origin of the A vectors. Thus, it follows that $A_{\max}\pm A_{\min}=(J+\frac{1}{2})P_l(\cos\theta)$, and if B can be neglected, then we have

$$b=\lambda^{-1}[(\sigma_{\max})^{\frac{1}{2}}\pm(\sigma_{\min})^{\frac{1}{2}}]=(J+\tfrac{1}{2})P_l(\cos\theta), \qquad (6)$$

where $\sigma_{\max}$ and $\sigma_{\min}$ are the maximum and minimum differential cross sections at the resonance. For Eq. (6) to be valid, the observed width of the resonance must be sufficiently small that the phase shifts of the partial waves which do not excite the resonance will be essentially constant as the energy is varied from the maximum to the minimum of the resonance.

Each scattering vector can be further broken down into two components which represent the "hard sphere" or normal potential scattering and the anomalous potential or resonance scattering. In some cases this breakdown of the scattering vectors will simplify the analysis, but in the discussion which follows, only the resultant of these two vectors will be drawn. Thus, each scattering vector corresponds to one of the terms in Eq. (2). For simplicity in the diagrams, the two scattering vectors for the lth partial wave ($l>0$) are sometimes combined to form one resultant vector. Reference to resonances and to the corresponding energy levels of the compound nucleus will be made in terms of symbols such as $P_{\frac{1}{2}}$. The subscript refers to the total angular momentum of the compound state, and the capital letter refers to the orbital angular momentum of the bombarding protons which form this state.

Sufficient data are not available from the present scattering experiment to carry out an accurate phase shift analysis. However, with the aid of a geometrical representation of the equations for scattering, some of the experimental results can be interpreted in a general manner. In order to apply the scattering equations it was necessary to make certain simplifying assumptions. The reaction radii are assumed to be independent of energy, and the reaction radii for all types of potential and resonance scattering except S scattering are assumed to be the same. These simplifications are probably not correct, but an accurate phase shift analysis would be necessary to determine what the properties of the reaction radii are.

III. THE 2.66-MEV RESONANCE

An analysis of the scattering data is most easily started in the low energy region of the curve because at low energies only the partial waves with low orbital angular momentum will contribute appreciably to the scattering. A convenient starting point for the present data is the 2.66-Mev resonance. Applying Eq. (6) to data on this resonance and using the cross section

TABLE I. Theoretical values for the diameters of the locus circles

Type of energy level	Diameter of locus circle $b=(J+\frac{1}{2})P_l(\cos 165°)$
$S_{1/2}$	1.00
$P_{1/2}$	0.97
$P_{3/2}$	1.93
$D_{3/2}$	1.80
$D_{5/2}$	2.70
$F_{5/2}$	2.41
$F_{7/2}$	3.22
$G_{7/2}$	2.74
$G_{9/2}$	3.42
$H_{9/2}$	2.74
$H_{11/2}$	3.28

[8] S. G. Kaufmann (unpublished) previously used a circular locus for plotting resonances where only interference between resonance and Rutherford-type scattering was considered.

values of the previous paper corrected to the center-of-mass system gives $b=1.12$ if the minus sign of Eq. (6) is used, and $b=2.05$ if the plus sign is used. The nature of the experimental cross section measurement is such that these values of b are not accurate, but they represent a maximum value for b. Table I gives the theoretical values for the diameters of the locus circles for the present experiment if the angular spread of the scattered protons which were detected is neglected. Averaging over the acceptance angle of the analyzer lowers slightly the theoretical diameters of the circles for the higher angular momenta.

A comparison of the experimental values of b with the theoretical values indicates that the only types of resonances which would give reasonable agreement are $S_{\frac{1}{2}}$, $P_{\frac{1}{2}}$, $P_{\frac{3}{2}}$, and $D_{\frac{3}{2}}$. A vector diagram was drawn for each of these four cases, and the shape of the resonance computed from the diagram was compared with the experimental results. The nearly symmetrical dip in the cross section was found to be reproduced theoretically only if the resonance is assumed to be $S_{\frac{1}{2}}$ and if a large phase shift for S-potential scattering is assumed at 2.66 Mev. Later attempts to explain the scattering data obtained from 0.6 to 2.66 Mev indicated that a large S-wave phase shift at 2.66 Mev was also a necessary consequence of a reasonable explanation of these data. The S-wave phase shift obtained from attempts to fit the low energy portion of the curve will be used in further discussion of the 2.66-Mev resonance.

Figure 2 shows the vector diagram for the 2.66-Mev resonance assuming it is an $S_{\frac{1}{2}}$ resonance. A vector drawn between points A and O would be the resultant of the D and P potential scattering and Rutherford scattering vectors, assuming a reaction radius of 5.31 $\times 10^{-13}$ cm and that there are no P or D resonances which influence the scattering at this energy. The vector OC represents the S wave scattering vector at an energy near the resonance but sufficiently far away so that the effect of the resonance is negligible. As the proton energy is varied over the resonance, the point C will move counterclockwise around the circle. Inspection of the vector diagram of Fig. 2 shows that the resonance indicated there will give a dip in the cross section which is nearly symmetric as was observed in the scattering experiment. Estimates were made of the effects of resonances above 2.66 Mev on the phase shifts at 2.66 Mev. These estimates were partially on the basis of the present experiment and partially on the basis of mirror level arguments. Consideration of the broad $P_{\frac{3}{2}}$ and $D_{\frac{3}{2}}$ levels at higher energies as well as a small contribution from F potential scattering at 2.66 Mev gives the vector BC of Fig. 2. The D potential scattering vector is broken down into its $D_{\frac{3}{2}}$ and $D_{\frac{5}{2}}$ components to show the effect of D resonances at higher energies on the scattering; and, similarly, the P vector is broken down into its $P_{\frac{1}{2}}$ and $P_{\frac{3}{2}}$ components. Figure 2 shows that resonances at higher energies will have only a small influence on the scattering at 2.66 Mev.

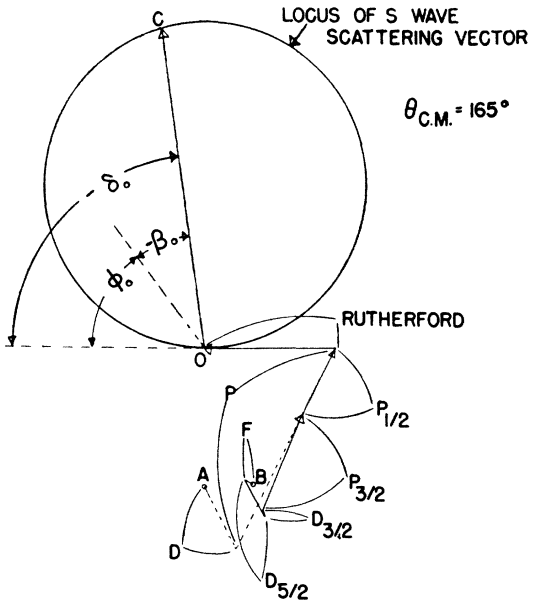

FIG. 2. Vector diagram for the scattering of 2.66-Mev protons from O^{16} through an angle of 165° in the center-of-mass system if an $S_{\frac{1}{2}}$ resonance is assumed at this energy.

The experimental diameter of the locus circle was 1.12, so that if the experimental data on the 2.66 Mev resonance is to be fitted to the theoretical curve for an $S_{\frac{1}{2}}$ resonance, the experimental cross sections must be multiplied by $1/(1.12)^2$. If the conversion from laboratory to center-of-mass system is also included in the factor, the experimental cross section values must be multiplied by 0.72; and in all further comparison of the formulas with experimental results the experimental cross sections will be multiplied by this factor. It should be recalled at this point that the experimental determination of the relative minimum cross section for the 2.66-Mev resonance was subject to a large percentage error. If the minimum were lower than the value used, it would be found that the point B in Fig. 2 would be closer to the locus circle than is shown, and the experimental cross section values would have to be multiplied by a factor smaller than 0.72. Also, moving the point B closer to the locus circle would enable this resonance to be explained with a smaller reaction radius for P and D scattering. Thus, the entire analysis presented here is indirectly dependent on the experimentally determined shape of the 2.66-Mev resonance. However, the general conclusions reached should not be dependent on these uncertainties.

Using the vector diagram of Fig. 2, a curve can be drawn which represents the theoretical shape of the resonance assuming it is $S_{\frac{1}{2}}$. Assuming a width, Γ, of 19.9 kev gave the best fit to the experimental data. A

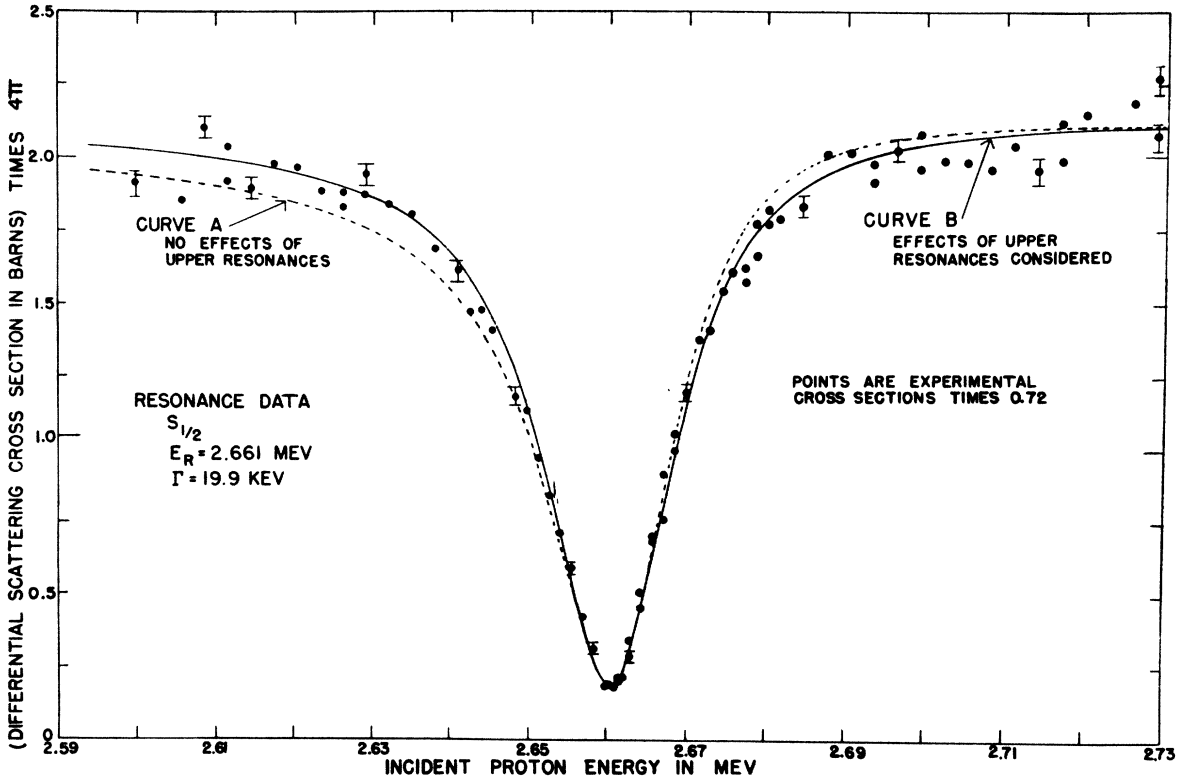

FIG. 3. Comparison of the theoretical shape of the 2.66-Mev resonance with the experimental points. The theoretical shape is based on the vector diagram of Fig. 2. Curve A corresponds to the vectors beginning at point A on Fig. 2 and curve B corresponds to the vectors beginning at point B on Fig. 2.

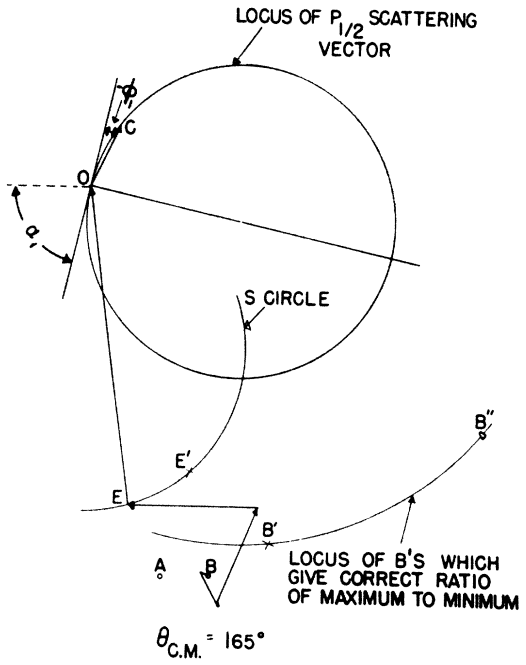

FIG. 4. Vector diagram for the scattering of 2.66-Mev protons from O^{16} through an angle of 165° in the center-of-mass system if a $P_{\frac{1}{2}}$ resonance is assumed at this energy.

comparison of the theoretical curves with the experimental points is shown in Fig. 3. The dashed curve A corresponds to the vectors which start at point A in Fig. 2, and the solid curve B corresponds to the vectors which start at point B in Fig. 2. It is seen that curve B, which takes into account the effect of resonances at higher energies, is a better fit to the experimental data.

If a $P_{\frac{1}{2}}$ resonance is assumed at 2.66 Mev, the vector diagram which is shown in Fig. 4 will be obtained. OC of Fig. 4 represents the $P_{\frac{1}{2}}$ vector off resonance, and EO represents the S wave scattering vector. For convenience, the $P_{\frac{1}{2}}$ vector has been moved to the position of the last vector of the sum. The same assumptions have been made in drawing Fig. 4 as were made for Fig. 2 except for the nature of the resonance. Points A and B of Fig. 4 correspond to the points A and B of Fig. 2. The $P_{\frac{1}{2}}$ locus circle is rotated through an angle of $(180°+\alpha_1°)$, where the extra 180° takes into consideration the fact that all odd legendre polynomials are negative for angles near 180°.

The shape of the 2.66-Mev resonance which results from the vector diagram of Fig. 4 is shown by the curve of Fig. 5 to be too asymmetric. This asymmetry can also be seen from the vector diagram. The locus of the points, B, on Fig. 4 which would give the correct ratio of maximum to minimum cross section is indicated

by the arc $B'B''$. The point B'' is the origin of the vector diagram which would give the experimentally determined shape to the cross section. No simple assumptions about neighboring resonances were found which could move the point B to B''. Moving B to B'' would require the presence of broad resonances near 2.66 Mev, which were not observed because of extremely unlikely interference effects. The arc labeled S circle is the locus of the point E as the S wave phase shift is varied while the point O is held fixed. It can be seen that decreasing the S wave phase shift also will not bring the point B to B''. On the basis of the vector diagram of Fig. 4 it has been concluded that the 2.66-Mev resonance is not $P_{\frac{1}{2}}$.

Vector diagrams for the 2.66-Mev resonance were also drawn assuming it to be $P_{\frac{3}{2}}$ or $D_{\frac{3}{2}}$. Arguments similar to those given above for the $P_{\frac{1}{2}}$ case can be used to rule out these other cases also. When the plus sign is used in Eq. (6), the start of the vector diagram must be inside the locus circle for the resonance. Because this condition is not fulfilled if a $D_{\frac{3}{2}}$ resonance is assumed,

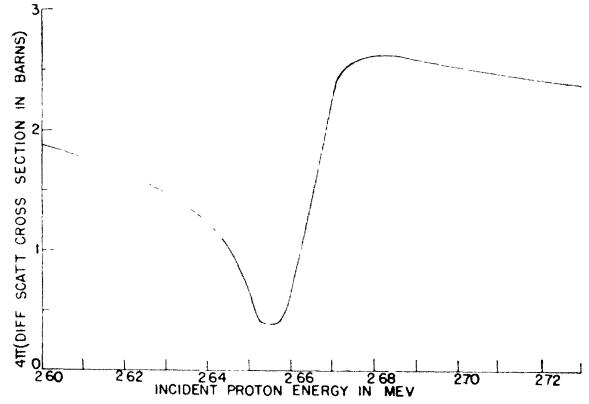

FIG. 5. Calculated shape of the 2.66-Mev resonance if it is assumed to be a $P_{\frac{1}{2}}$ resonance. Calculations are based on the vector diagram of Fig. 4.

this possibility is readily eliminated without additional arguments.

If the analysis of the 2.66-Mev resonance presented above is correct, it should be possible to predict results of other experiments on the scattering of protons in this energy region by oxygen. The simplest experimental method determining the validity of the above analysis would probably be a determination of the shape of the 2.66-Mev resonance when protons scattered through 90° in the center-of-mass system are observed. Figure 6 shows the vector diagram for scattering through 90°, assuming the 2.66-Mev resonance is $S_{\frac{1}{2}}$. OC represents the S wave scattering off resonance, and various S wave vectors for energies in the resonance region are shown by dashed lines. It should be noted that P scattering does not contribute at 90° if there is no P resonance. The predicted shape of the 2.66-Mev resonance if observed at 90° is shown by the upper curve of Fig. 7,

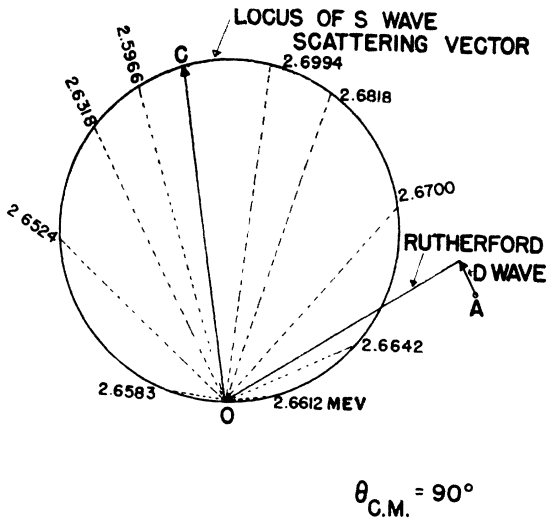

FIG. 6. Vector diagram for the scattering of 2.66-Mev protons from O^{16} through an angle of 90° in the center-of-mass system. The same assumptions have been made for this diagram as for curve A of Fig. 3. The S-wave scattering vectors at various energies are indicated by dashed lines.

which was drawn by the use of the vector diagram of Fig. 6. If a P resonance is assumed, only factor B of Eq. (1) will contain a term due to the resonance, and

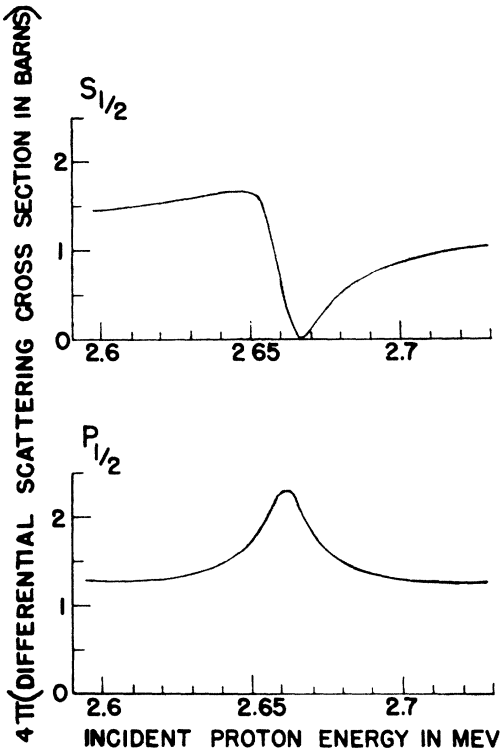

FIG. 7. A comparison of the calculated shape of the 2.66-Mev resonance for scattering through a center-of-mass angle of 90° if either an $S_{\frac{1}{2}}$ or a $P_{\frac{1}{2}}$ resonance is assumed. The $S_{\frac{1}{2}}$ curve is obtained from the vector diagram of Fig. 6. The $P_{\frac{1}{2}}$ curve is obtained using the same parameters except for the type of resonance assumed.

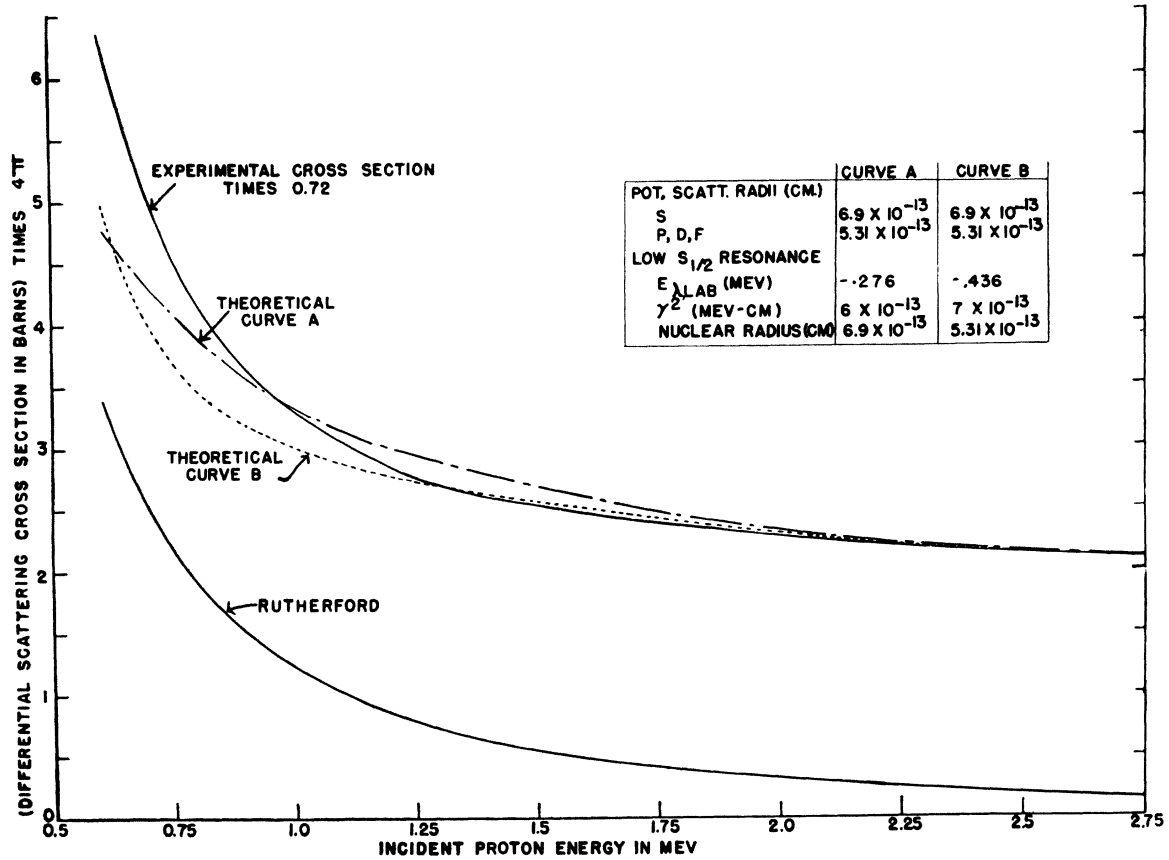

FIG. 8. A comparison of the experimental yield curve for scattering at low energies with curves calculated using assumed values for the nuclear parameters. Calculations are based on scattering through 165° in the center-of-mass system. The 2.66-Mev resonance is not shown on these curves because this resonance is narrow and will influence the scattering only in the neighborhood of the resonance.

the shape will be as shown by the lower curve of Fig. 7. A $P_{\frac{1}{2}}$ or a $P_{\frac{3}{2}}$ resonance appears the same if protons scattered through 90° are observed. Figure 7 shows a marked difference between the calculated shapes of an S or a P resonance when the angle of observation is 90°.

It can be seen from the vector diagram of Fig. 6 that if the ratio of maximum to minimum cross section at 90° can be experimentally determined, then the D wave contribution at 2.66 Mev can easily be calculated (assuming an $S_{\frac{1}{2}}$ resonance). By using relatively simple techniques such as this, it should be possible to lessen the complications involved in an analysis of experimental scattering data.

IV. ELASTIC SCATTERING AT ENERGIES BELOW 2.66 MEV

The outstanding feature of the low energy scattering data is that the cross section is larger than the Rutherford cross section and decreases with increasing energy much more slowly than does the Rutherford cross section. The low energy data can be explained in a general manner by assuming the existence in the compound nucleus of a broad $S_{\frac{1}{2}}$ level at low energies. A P or higher order level will not explain the large cross sections over an extended low energy region because the penetrabilities of these partial waves are too small at low energies. With the information available, the only method of analyzing the low energy data was to assume values of the parameters involved and then compare the calculated curve with experiment. The two best fits to the experimental curve which were obtained after a small number of trials are shown in Fig. 8. The 2.66-Mev resonance is not shown on the curve, because it is narrow and will effect the scattering only in the immediate neighborhood of the resonance.

Some time after the calculations indicated in Fig. 8 were finished, the existence of a low-lying level in F^{17} was established by Ajzenberg,[9] who observed neutrons from the $O^{16}(d,n)O^{17}$ reaction. The position of the level was found to be 551±15 kev above the ground state rather than at 350 kev or 200 kev, which were used in Fig. 8 for curves A and B, respectively. The assumption of a bound level was correct. Recalculation of the curves in Fig. 8 does not seem profitable until more experimental information is available on the scattering of protons by oxygen in the low energy region. Some evi-

[9] F. Ajzenberg, Phys. Rev. **83**, 875 (A) (1951).

dence is also presented by Ajzenberg to show that the low-lying level is $S_{\frac{1}{2}}$, in agreement with the assumptions made for analyzing the present experiment.

It has been shown by Thomas[6] that in calculations of scattering cross sections where a broad resonance influences the scattering, the variation of Δ_λ with energy must be considered. If a resonance is narrow, such as the one at 2.66 Mev, then Δ_λ for this level can be assumed to be constant and $(E_\lambda+\Delta_\lambda)$ may be taken as the resonance energy, E_R. For calculations involving the low energy scattering data, the variation of Δ_λ with energy has been considered. Δ_λ is a sum of the values of Δ for the various modes of decay of the compound state λ. In the present experiment gamma-ray emission and proton emission are the only two possible modes of decay of the compound nucleus, and the Δ for gamma-ray emission is small in comparison with that for proton emission. Hence, only the value of Δ for proton emission has been given in Eq. (5) for Δ_λ, and this value was used in the calculations. If the formulas used in this paper are correct, then the 0.55-Mev level in F^{17} has a very peculiar property. This level is a bound level and can decay only by gamma-ray emission so that observation of the level by the $O^{16}(d,n)O^{17}$ reaction should give very nearly the value of E_λ. As the binding energy of oxygen for a proton is 0.61 Mev, E_λ will be -0.06 Mev referred to the center-of-mass system. The value of Δ_λ for low energy S protons will be positive and sufficiently large so that there will exist a proton energy, E_R, for which $(E_\lambda+\Delta_\lambda)=E_R$. For proton energies in the immediate vicinity of E_R, the scattering cross section will behave in an anomalous manner typical of a resonance, although the cause of this behavior is a bound energy level. Experimental data on the scattering of low energy protons by oxygen are needed in order to determine the validity of the above arguments.

Attempts to fit the low energy scattering data of the present experiment have led to the conclusion that the reduced width of the low lying level is near the maximum allowed by Wigner's criterion,[10] which states that the maximum value of the reduced width is given approximately by the relation,

$$\gamma_\lambda^2 \simeq \tfrac{3}{2}\hbar^2/mR, \qquad (7)$$

where m is the reduced mass of the system, $\hbar$ is Planck's constant divided by 2π, and R is the reaction radius. All assumptions which were made for the calculations in the low energy region were limited in two respects: (1) to values of γ_λ^2 which obey Wigner's criterion, and (2) to combinations of E_λ, γ_λ^2, and R which give $(E_\lambda+\Delta_\lambda)_{E=E_R}<450$ kev, as was observed experimentally.

Rather large reaction radii have been used in the calculations because they appeared to be necessary in order to fit the experimental data. More accurate and extensive data are needed to obtain accurate values for the reaction radii. Smaller values for the absolute cross sections will lead to somewhat smaller reaction radii. Results of the analysis presented indicate that the reduced width of the F^{17} levels can vary over a wide range. The reduced width of the 3.11-Mev $S_{\frac{1}{2}}$ level is 0.048×10^{-13} Mev-cm, while the 0.55-Mev $S_{\frac{1}{2}}$ level appears to have a reduced width at least 100 times larger. Perhaps this difference in the reduced widths is caused by a fundamentally different mode of excitation for the two states.

[10] E. P. Wigner, Am. J. Phys. **17**, 99 (1949).

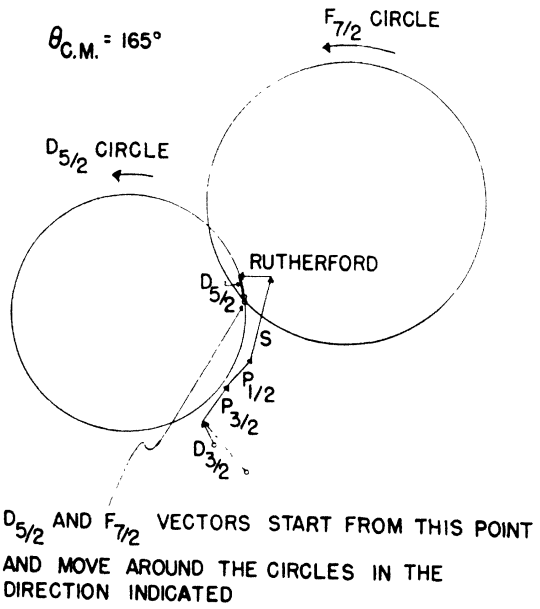

FIG. 9. Vector diagram for the scattering of 3.47-Mev protons from O^{16} through an angle of 165° in the center-of-mass system. The locus circles for both a $D_{5/2}$ and an $F_{7/2}$ resonance at this energy are also shown.

V. THE SCATTERING DATA AT ENERGIES ABOVE 2.66 MEV

If the best experimental values obtained for the 3.47-Mev resonance are substituted in Eq. (6), the result is $b=3.1$ using the minus sign or $b=4.4$ using the plus sign. These values may be low because of the difficulty in obtaining a sufficiently small proton beam spread to determine the true shape of this very narrow resonance. The value of $b=4.4$ can be ruled out immediately because it is larger than any of the possible values of b given in Table I. In order to decide between the several assignments which may be made to the 3.47-Mev resonance on the basis of Eq. (6), the vector diagram shown in Fig. 9 was drawn together with a circular locus for either a $D_{\frac{1}{2}}$ or an $F_{7/2}$ resonance.

It will be assumed in the discussions which follow that the parity of an energy level of F^{17} is equal to the parity of the orbital angular momentum of the proton which interacts with O^{16} to form the energy level. For convenience, a resonance will be said to have even or odd parity depending on whether the orbital angular momentum of the protons which excite the resonance have even or odd parity.

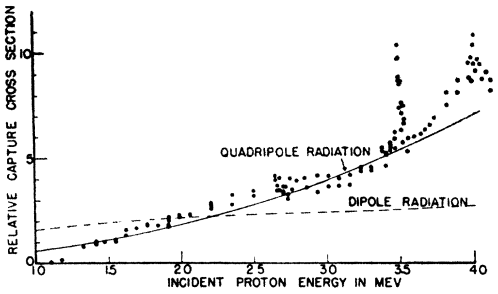

FIG. 10. Comparison of the calculated variation of the capture cross section with the experimental points. Calculations are shown for two possible modes of decay of the compound state, and they assume that the capture is caused by the broad low energy level of F^{17}. No account has been taken of the resonance at a proton energy of 3.99 Mev. The nuclear parameters assumed for curve B of Fig. 8 have been used for the calculations. The curves were normalized to the experimental data at the following points: dipole radiation, 2 Mev; quadrupole radiation, 3 Mev.

All locus circles for even parity resonances caused by D or higher order partial waves would have approximately the same position on Fig. 9 because values of α_l are not sensitive to the value of l for the larger values of l. Similarly, all locus circles for odd parity resonances caused by F or higher order partial waves will have approximately the same position. An inspection of the vector diagram at 3.47 Mev shows that an even parity resonance would give a yield curve exhibiting the maximum cross section at a lower energy than the minimum. However, an odd parity resonance would have the minimum cross section at a lower energy than the maximum. The experimental curve fits the latter case; and, therefore, the 3.47-Mev resonance was taken to be an F or higher order resonance of odd parity. On the assumption that an H resonance would not be expected until higher energies were reached, the resonance at 3.47 Mev was taken to be excited by F protons. The experimental value of b leads to a choice of 7/2 rather than 5/2 as the total angular momentum of the compound state.

The best experimentally determined shape of the 3.47-Mev resonance indicates that if this resonance is $F_{7/2}$, the vector diagram should begin at the point marked by an x in Fig. 9. Resonances at higher energies will have an effect on the 3.47-Mev vector diagram because of the relatively high penetrability of P and D partial waves at this and higher energies. Although the effect of these resonances was estimated for the diagram shown, their influence may be larger than this estimate, and in this case the start of the vector diagram will move toward the point x. The effect of increasing the assumed width of a higher energy $D_{\frac{3}{2}}$ resonance is shown by the dotted $D_{\frac{3}{2}}$ vector in Fig. 9. No reasonable assumptions would enable the vector diagram to indicate an even parity resonance.

If the slowly rising scattering cross section between 3.5 and 4.0 Mev is attributed to the 3.99-Mev resonance, which was indicated by the capture data, then this resonance is of the type which would give a maximum before the minimum. Since the arguments about even and odd parity resonances which were used at 3.47 Mev apply to this case also, the resonance is assumed to be even parity. Mirror level arguments indicate that the total angular momentum should be $\frac{3}{2}$, and hence the assignment $D_{\frac{3}{2}}$ is given to the 3.99-Mev resonance.

If the minimum at 4.26 Mev and the maximum near 4.5 Mev in the scattering yield curve are caused by the same resonance, then b is calculated to be 1.8 or 5.0 using the minus or plus sign, respectively, of Eq. (6). It is assumed that Eq. (6) can be applied in this instance to indicate the value of J, in spite of the interference between resonances, because the variation of the $D_{\frac{3}{2}}$ vector due to the 3.99-Mev resonance is not large between 4.27 and 4.5 Mev. A comparison of the experimental values of b with Table I indicates that the total angular momentum is probably $\frac{3}{2}$. Mirror level arguments indicate that the 4.39-Mev resonance is $P_{\frac{3}{2}}$.

The above discussion explains the general shape of the scattering yield curve at high energies. However, when a detailed theoretical calculation of the shape of the curve was made, it was found that the general level of the experimental cross section above about 3.7 Mev was higher than could be accounted for by the resonances discussed above. This is probably to be expected, since in this energy region penetrabilities of high order partial waves are relatively high, and the observed widths of resonances can be very large. Broad resonances probably occur at energies slightly higher than were reached in the present experiment, and the effects of these resonances may be large above 3.7 Mev.

Effects of the ground state of F^{17} on the scattering have been neglected in the analysis described here. There is evidence that the ground state is $D_{\frac{5}{2}}$, and if the $D_{\frac{3}{2}}$ resonance at 3.99 Mev is caused by a level which forms an inverted doublet with the ground state, then the reduced width of the ground state may be assumed to be large. Below 2.66 Mev the penetrability of D waves is so small that the ground state will have only a small effect on the scattering. At higher energies the influence of the ground state may be large. The start of the 3.47-Mev vector diagram of Fig. 9 would be closer to that expected from the experimental shape of the curve, and the calculated general level of the cross section over the high energy portion of the yield curve would be raised if the effects of a D ground state were included.

VI. ANALYSIS OF THE CAPTURE DATA

The peak observed in the capture cross section near 3.47 Mev can easily be explained by the narrow 3.47-Mev resonance observed in the scattering yield. The large capture cross section which extends over the entire energy range is probably caused by the broad $S_{\frac{1}{2}}$ level in F^{17}. A comparison of the calculated variation of the capture cross section with the experimental points is shown in Fig. 10. The calculated variation is based

on the one-level dispersion formula[11] in the following form:

$$\sigma=\pi\lambda^2\Gamma_\gamma\Gamma_p/[(E_\lambda+\Delta_\lambda-E)^2+\tfrac{1}{4}\Gamma^2],$$

where $\Gamma_p=[2k\gamma_\lambda^2/(F_l^2+G_l^2)]_{r=Rl}$ is the width of the level for proton emission, Γ_γ is the width of the level for gamma-ray emission, and $\Gamma=\Gamma_p+\Gamma_\gamma$. Since Γ_γ is small compared with Γ_p, Γ can be taken as equal to Γ_p. The characteristics of the low-lying F^{17} level which were assumed for curve B of Fig. 8 have been used for the calculated curves of Fig. 10, and the experimental points are those obtained with the thin oxide targets. The variation of Γ_γ with energy will depend on the type of gamma-radiation by which the compound nucleus decays. For dipole radiation, Γ_γ will be proportional to the cube of the gamma-ray energy, while for quadrupole radiation, Γ_γ will be proportional to the fifth power of the gamma-ray energy. The calculated curve of Fig. 10 for dipole radiation was normalized to the experimental data at 2.0 Mev, and the normalization point for the quadrupole radiation curve was at 3.0 Mev.

Figure 10 shows that the capture cross section extending over a large energy region can be explained on the basis of the low-lying level in F^{17}. The large departure of the experimental points from the theoretical curve for quadrupole radiation in the energy range above 3.7 Mev probably results from the broad resonance at 3.99 Mev which was not considered in the calculations. The reasonably good agreement between the curve for quadrupole radiation and the experimental points is an indication that quadrupole radiation is the mode of transition from the low lying $S_{\frac{1}{2}}$ level to the ground state. It is possible, however, that the curve for dipole radiation would fit the experimental points if the possible variation of the nuclear matrix elements with energy could be taken into account.

If it is assumed that quadrupole radiation is responsible for the capture by the broad $S_{\frac{1}{2}}$ level, then some statements about the ground state of F^{17} can be made. It will be assumed that this ground state has even parity and is either an S or a D state. Shell models of the nucleus[1,2] eliminate a P ground state. If the ground state were $S_{\frac{1}{2}}$, then magnetic dipole radiation would be allowed, and the calculated curve for dipole radiation should fit the experimental points. If the ground state were $D_{\frac{1}{2}}$, electric quadrupole or higher order radiation would be required, as is indicated by the present data. A $D_{\frac{1}{2}}$ ground state could be reached from the $S_{\frac{1}{2}}$ level by either magnetic dipole or electric quadrupole radiation. According to a paper by Austern and Sachs,[12] the magnetic dipole radiation should predominate in this case, and the behavior of the cross section would then be expected to follow that for dipole radiation. Thus, the variation of the capture cross section with energy gives some evidence, but is not proof, that the ground state of F^{17} is $D_{\frac{1}{2}}$.

A $D_{\frac{1}{2}}$ ground state can be reached from the $F_{7/2}$ level by electric dipole radiation, which is more likely to give the large peak in the capture cross section at 3.47 Mev than an electric octupole transition, which would be required if the ground state were $S_{\frac{1}{2}}$.

VII. COMPARISON OF THE ENERGY LEVELS IN THE MIRROR NUCLEI, F^{17} AND O^{17}

A summary of the energy levels assigned to F^{17} is shown on Fig. 11 together with the energy levels in O^{17} for comparison. The O^{17} and F^{17} energy level diagrams have been shifted so that their ground states coincide on the vertical energy scale. A detailed list of reactions leading to excited states of O^{17} together with references is given by Hornyak *et al.*[13] In light of more recent experiments, some changes have been made in the energy level diagram for O^{17} which is given in this review. The positions of the 4.56-, 5.08-, and 5.36-Mev energy levels in O^{17} were obtained from the experiments of Bockelman[14] on the scattering of neutrons by oxygen. The positions of the other energy levels of O^{17} have been taken from the work of Rotblat,[15] although it should be mentioned that the position of the 0.87-Mev level has been located by other more accurate experiments.

Experiments by Burrows *et al*[16] on the angular dis-

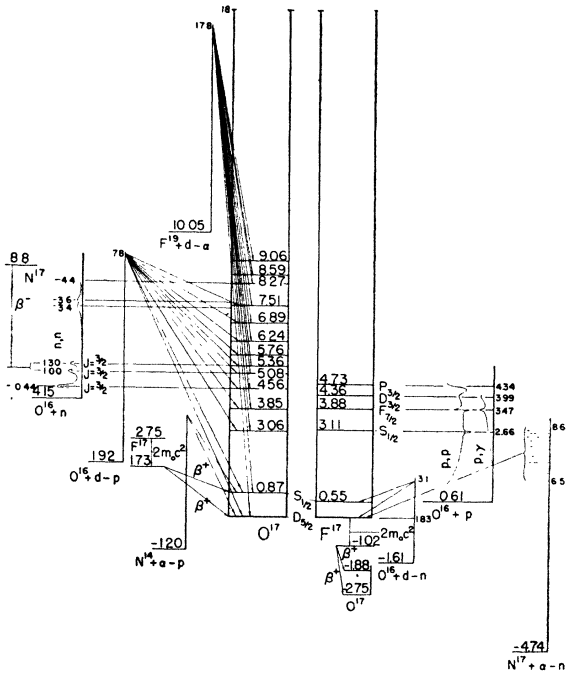

FIG. 11. Comparison of the energy levels in the mirror nuclei, O^{17} and F^{17}.

[11] E. P. Wigner and L. Eisenbud, Phys. Rev. **72**, 29 (1947).
[12] N. Austern and R. G. Sachs, Phys. Rev. **81**, 710 (1951).
[13] Hornyak, Lauritsen, Morrison, and Fowler, Revs. Modern Phys. **22**, 291 (1950).
[14] C. K. Bockelman, Phys. Rev. **80**, 1011 (1950).
[15] J. Rotblat, private communication, courtesy of T. Lauritsen.
[16] Burrows, Gibson, and Rotblat, Phys. Rev. **80**, 1095 (1950).

TABLE II. Calculated widths Γ_p of the F^{17} levels which correspond to levels of O^{17}.

O^{17} energy level Mev	Observed resonance energy for $O^{16}(n,n)$ reaction	Observed width, Γ_n Mev in the lab system	Assumed reaction radius cm	$P_{\frac{1}{2}}$ level assumed γ^2 Mev-cm	$P_{\frac{1}{2}}$ level assumed Γ_p calculated for 4-Mev protons Mev	$D_{\frac{3}{2}}$ level assumed γ^2 Mev-cm	$D_{\frac{3}{2}}$ level assumed Γ_p calculated for 4-Mev protons Mev
4.56	0.44	0.053	3.78×10^{-13}	0.79×10^{-13}	0.26	21.0×10^{-13}	1.9
5.08	1.00	0.100	3.78×10^{-13}	0.57×10^{-13}	0.18	5.9×10^{-13}	0.52
5.36	1.30	0.040	3.78×10^{-13}	0.17×10^{-13}	0.055	1.3×10^{-13}	0.12
4.56	0.44	0.053	5.31×10^{-13}	0.49×10^{-13}	0.24	6.1×10^{-13}	1.4
5.08	1.00	0.100	5.3×10^{-13}	0.39×10^{-13}	0.19	2.0×10^{-13}	0.45
5.36	1.30	0.040	5.3×10^{-13}	0.12×10^{-13}	0.06	0.46×10^{-13}	0.10

tribution of protons from the $O^{16}(d,p)O^{17}$ reaction have been interpreted by Butler[17] to indicate that the ground state of O^{17} is a D state, and the 0.87-Mev level is an $S_{\frac{1}{2}}$ state. A recent measurement of the spin[18] of O^{17} gives the value 5/2, so that the ground state is probably $D_{\frac{5}{2}}$. It therefore appears as if the ground state and first excited state of O^{17} have the same total angular momentum and parity as the corresponding states of F^{17}.

The 3.06- and 3.85-Mev levels in O^{17} correspond in position with the 3.11- and 3.88-Mev levels in F^{17}. No further information is available on the characteristics of these O^{17} levels, so that a more detailed comparison cannot be made.

Experiments on the scattering of neutrons by oxygen[14] indicate that the angular momentum of the 4.56-, 5.08-, and 5.36-Mev levels of O^{17} is $\frac{3}{2}$ in each case. This agrees with the angular momentum of $\frac{3}{2}$ found for the 4.73-Mev level in F^{17}. In order to compare the results of the proton scattering experiment with what would be expected on a mirror level hypothesis, Table II was calculated. This table gives the observed widths, Γ_p, of the F^{17} levels which correspond to the 4.56-, 5.08-, and 5.36-Mev O^{17} levels if the following assumptions are made: (1) Corresponding O^{17} and F^{17} levels have the same reduced widths, (2) the same reaction radii can be used for neutron and for proton scattering, (3) all F^{17} levels are observed by the scattering of 4-Mev protons. The latter assumption was made for convenience in the calculations and was allowable because the penetrabilities for P or D waves do not vary greatly over the range from 4.0 to 4.5 Mev. Table II gives results of the calculations for two different reaction radii and for either a $P_{\frac{1}{2}}$ or a $D_{\frac{5}{2}}$ assignment to each level. Values of the reduced widths of the levels are also given, and these may be compared with the maximum values of approximately 18×10^{-13} Mev-cm and 13×10^{-13} Mev-cm allowed by Wigner's criterion for reaction radii of 3.78×10^{-13} cm and 5.31×10^{-13} cm, respectively.

From the proton scattering data, Γ_p for the 4.73-Mev level in F^{17} is estimated to be about 0.24 Mev, and fitting this value to the data of Table II indicates that reasonable agreement is obtained only if the level is assumed to be $P_{\frac{1}{2}}$. Table II indicates that the 4.73-Mev level of F^{17} may correspond to either the 4.56- or 5.08-Mev level of O^{17}. While agreement appears better with the 4.56-Mev level, the possibility of a larger reaction radius for proton scattering than for neutron scattering could give a good correspondence with the 5.08-Mev level.

The value of Γ_p for the 4.36-Mev level in F^{17} cannot be reliably obtained from the available data, but the best estimate from the capture data gives $\Gamma_p\cong0.5$ Mev for this level. This estimate takes into consideration the effect of the variation of Δ_λ with energy in making the actual observed width less than Γ_p. A comparison with Table II indicates that this 4.36-Mev level is $D_{\frac{3}{2}}$ and probably corresponds to the 5.08-Mev level of O^{17}. This assignment is in agreement with the D assignment made previously on the basis of the proton scattering data. The two highest levels observed in F^{17} appear, therefore, to have similar characteristics to two mirror levels in O^{17}, although the levels do not appear in the same order in F^{17} as in O^{17}.

In view of the fact that the $D_{\frac{3}{2}}$ level has a large reduced width, the relatively large downward shift of the $F^{17}D_{\frac{3}{2}}$ level with respect to the corresponding $O^{17}D_{\frac{3}{2}}$ level might be expected. The 3.11- and 3.88-Mev levels in F^{17}, which correspond very closely in energy to their mirror levels in O^{17}, have small reduced widths.

The value of Δ_p for the 4.36-Mev F^{17} level cannot be obtained from the present data with sufficient accuracy to rule out the equivalence of this level with the 4.56-Mev level in O^{17}. If the 4.56-Mev O^{17} level is a $D_{\frac{5}{2}}$ level, then Table II indicates that the reduced width of this level is very large. It would be necessary to assign a large reaction radius to the scattering if Wigner's criterion is to be obeyed.

A comparison of the energy levels of O^{17} and F^{17} is very favorable to the mirror nucleus hypothesis.

The authors wish to thank Professor R. G. Herb, under whose supervision this project was carried out, for his assistance and encouragement. Very valuable discussions with Professor H. T. Richards, Dr. R. K. Adair, and Dr. F. P. Mooring are also gratefully acknowledged.

[17] S. T. Butler, Phys. Rev. **80**, 1095 (1950).
[18] F. Alder and F. C. Yu, Phys. Rev. **82**, 105 (1951).